

Self-organized magnetic particles to tune the mechanical behaviour of a granular system

Meredith Cox,¹ Dong Wang,¹ Jonathan Barés,¹ and Robert P. Behringer¹

¹*Department of Physics & Center for Nonlinear and Complex Systems,
Duke University, Durham, North Carolina 27708, USA*

(Dated: November 9, 2015)

Above a certain density a granular material jams. This property can be controlled by either tuning a global property, such as the packing fraction or by applying shear strain, or at the micro-scale by tuning grain shape, inter-particle friction or externally controlled organization. Here, we introduce a novel way to change a local granular property by adding a weak anisotropic magnetic interaction between particles. We measure the evolution of the pressure, P , and coordination number, Z , for a packing of 2D photo-elastic disks, subject to uniaxial compression. Some of the particles have embedded cuboidal magnets. The strength of the magnetic interactions between particles are too weak to have a strong direct effect on P or Z when the system is jammed. However, the magnetic interactions play an important role in the evolution of latent force networks when systems containing a large enough fraction of the particles with magnets are driven through unjammed states. In this case, a statistically stable network of magnetic chains self-organizes and overlaps with force chains, strengthening the granular medium. We believe this property can be used to reversibly control mechanical properties of granular materials.

Keywords: Granular materials, Magnetic particle, Self organization, Jamming transition, Smart fluid

Above a certain density granular materials jam [1]. As the medium transitions from unjammed to jammed, its behavior changes from fluid-like to solid-like. This property, which is often a drawback in a silo or in a funnel, has been used recently for innovative architecture constructions [2] and soft robotic actuators [3–5]. In these cases, system parameters are tuned to reversibly change a soft material into a solid and strong one. There are at least two ways to reach this goal [6]: (i) macroscopically: one can act on the material boundaries to change the system volume/density [3], or one can apply system-wide shear strain; (ii) locally: one can change grain shapes [7, 8], local organization [2], or friction. These different approaches can be used to stabilize or destabilize the granular packing. Reversibly changing the system properties at the global scale is routine, but changing properties at the grain scale is much more challenging. We take a first step toward a novel manner to affect the macroscopic behavior of a granular packing by changing grain-scale properties. We do so by the addition of magnets to a controlled fraction of the grains. The magnetic interaction strength at the local scale is very weak compared to interaction forces that are typical of jammed states. Despite the low magnetic forces involved, the fluidity of the granular system below jamming, provides a mechanism for self-organization of structures that is reminiscent of magneto-rheological fluids [9–11].

The experiment consists of uniaxial compression (see Fig.1-(a)) of a mixture of 645 bidisperse (60% small, 40% large) photo-elastic disks with either diameter 12.7 or 15.9 mm, and thickness 6 mm. This ratio prevents crystalline ordering. A $4 \times 4 \times 4 \text{ mm}^3$ neodymium magnet was embedded in the bottom of a fraction R_m of the disks as in Fig.1-(b), and a UV-fluorescent bar was drawn

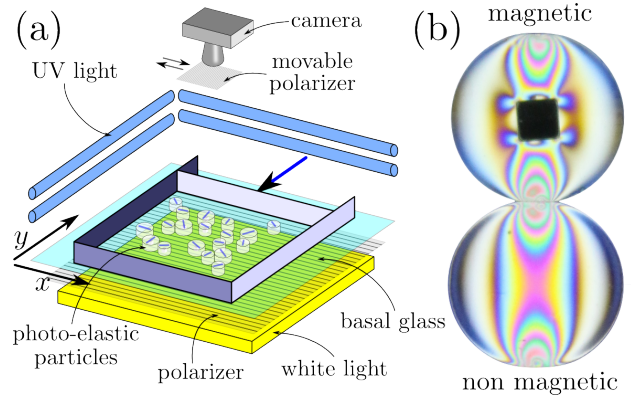


FIG. 1. (color online) (a): 3D schematic of the uniaxial compression experiment. A moving wall (blue arrow) compresses bidisperse magnetic photo-elastic particles by small steps. Each particle is marked on top by a bar, drawn in UV-fluorescent ink that gives the orientation of the embedded magnet. At each step the system is imaged in white light, (i) between crossed polarizers, (ii) without crossed polarizers, and (iii) in UV light. (b): top view with crossed polarisers showing magnetic and non-magnetic particles that have been compressed uniaxially. The presence of an embedded magnet modifies the inner mechanical and photoelastic response of a particle.

along the attractive direction of the magnet on the top of each particle. The particles were cast in a reverse-image chemically-resistant silicone [12] mold that was formed over a high resolution 3D printed base. The disks were cast from shore stiffness 50 liquid polyurethane [13] and then cured. For some particles, a magnet was centered at the bottom of the mold before pouring the polyurethane; this process avoided residual stresses around the magnet

in the unstressed state. The friction coefficient between particles is 0.62 ± 0.07 .

The disks were placed in a $44 \times 40 \text{ cm}^2$ (x, y) rectangular cell, in a spatially random stress-free compact rectangle with the long direction corresponding to the direction of compression. Initially, there was a $\sim 3\text{cm}$ gap between the particles and the cell boundaries. The particles rested on a smooth Plexiglas[®] sheet lubricated with talc, yielding a particle-base friction coefficient of 0.36 ± 0.04 . The setup was illuminated from below by a circular polarized uniform white light source, and from above by less intense UV lights. A 20 megapixel SLR camera, mounted 2 m above the particles, recorded views with and without a crossed (with respect to the source) circular polarizer (see Fig.1-(a)). After each 1mm compression step, the system was imaged a) without the second polarizer, b) with the second crossed polarizer (see Fig.1-(b)), and c) with the white light off and UV light on. The normal light pictures gave the particle positions. The UV light pictures gave the magnetic orientations. The pressure inside each disk (see inset of Fig.3) was computed from the squared gradient of the photo-elastic image intensity G_m^2 (for magnetic particles) and G_{nm}^2 (for non-magnetic particles) following [14–17]. The $P \sim G^2$ values were corrected using the inset graph of Fig.2 to account for differences in the different particle types, as suggested by Fig.1-(b). That is, the calibration between squared gradient and P is different for magnetic, G_m , and non-magnetic, G_{nm} , particles primarily because the stiff magnet deforms the photo-elastic response. Contacts between particle are also accurately detected (see inset of Fig.3) using positions and the photo-elastic response, as in Majmudar et al. [18]. The sensitivity of the polyurethane permits us to observe a photo-elastic response of the particles for applied forces as low as 0.015N. This is sufficient sensitivity to allow the detection of contacts due to magnetic attraction of the particles.

The inter-particle interaction forces have been measured for pulling and pushing different combinations of disks (small/large/magnetic/non-magnetic) away/toward each other and measuring the resulting force f and edge-to-edge distance between disks δ in a micro-strain analyser (TA Instruments RSA III). Fig.2 shows that during compression, magnetic and small particles are stiffer. In every case the particles exhibit Hertzian-like behavior and the magnetic attractive forces follow $f \sim -e^{-0.35\delta}$. Also, the highest attractive magnetic forces (0.05N) are greater than forces due to basal friction ($\sim 0.005\text{N}$), and both are much lower than repulsive forces measured in strong force chains ($\sim 2\text{N}$). This implies the magnetic forces cannot play a direct role in the modification of the macroscopic behavior of the granular material, once it is jammed.

However, the magnetic particles clearly influence the evolution of the system and the medium response. Fig.3-(a) shows the evolution of the global pressure computed

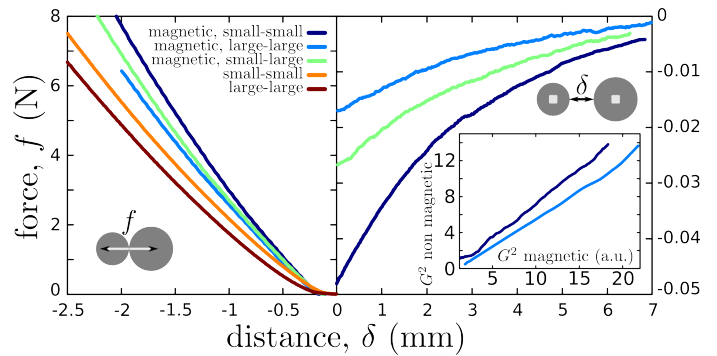


FIG. 2. (color online) Details of interactions between particles. For the different combination of particles (small/large/magnetic/non-magnetic) the interaction force is plotted as a function of distance δ or overlap ($\delta < 0$) between particle boundaries. Force scale for positive δ (right panel) is not the same as for negative (left panel). Non-magnetic particles are slightly softer than magnetic once. For the latter, a maximum attractive force of 0.05N is measured. Inset: for an equal compression force, G^2 (averaged over all pixels inside the photo-elastic materials of the particle) is plotted for magnetic G_m^2 and non-magnetic G_{nm}^2 particles, for small and large particles. A linear variation is found: $G_m^2 = k \cdot G_{nm}^2$ with $k > 1$.

as the sum of G^2 over all the disks when the granular system is compressed for different magnetic particle ratios R_m , from 0% (no magnetic particles) to 100% (only magnetic particles). Each curve represents an average over three compression runs. Two different responses arise, one for low R_m and another for high R_m . The data for $R_m = 0\%$ is characteristic of all the lower R_m response curves, and $R_m = 100\%$ is characteristic of the higher R_m responses. In the first case, P stays around zero, and in response to strain, particles just rearrange to relax the system like a liquid; P then increases rather rapidly above a critical-like ε . In the second case, pressure increases more rapidly with ε , and the sharp increase occurs at a lower ε somewhat like a plastic material.

The distinction between low and high R_m is particularly dramatic for the evolution of Z vs. ε , or packing fraction ϕ , for different ratios of magnetic particles. As in Fig.3 (b), for $R_m < 50\%$, and as previously observed in [18] for purely non-magnetic systems, Z is initially very low ($Z < 1$) and increases over a modest range of compressions to the jamming point $Z = 3$ which corresponds to the sharp increase in P . In contrast, when $R_m > 50\%$ the coordination number is always higher than in the non-magnetic case due to contacts caused by magnetic attraction, which leads to $Z \simeq 2$. Then, when the system is compressed, Z increases roughly linearly until the rate of increase accelerates after crossing the jamming point. As with P , the responses are either nearly the same for all ($R_m < 50\%$) or all similar for all ($R_m > 50\%$), with a rapid crossover for $R_m \simeq 50\%$. We believe this is due to a percolation transition for magnetic chains we

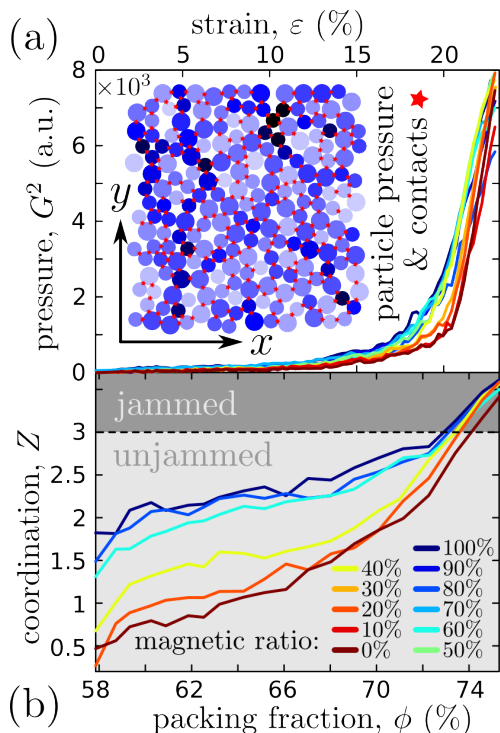


FIG. 3. (color online) Evolution of the pressure, measured as corrected G^2 (a) and of the coordination number, Z (b) as a function of the applied strain ε and of the packing fraction ϕ for different ratios of magnetic particles, from 0% (only non-magnetic) to 100% (only magnetic). The higher the percentage of magnetic particles, the stiffer the system and the faster pressure increases. The number of contact per grains is naturally higher for magnetic particles and the system jams faster. In (b) a dashed line for $Z = 3$ marks the jamming transition. (a)-inset: part of the system for a 100% magnetic particle experiment at $\varepsilon = 0.21$; darkness of the particle shows the pressure (from light–low pressure to dark–high pressure); red stars stands for contacts.

will describe later. The jamming packing fraction, ϕ_J , shifts from ~ 0.728 when the system is purely magnetic to ~ 0.742 when the system is completely nonmagnetic. Note that all the jamming points are significantly lower than 0.84, the isotropic jamming point in 2D, because uniaxial compression is anisotropic, and friction between particles allows for shear jamming (note that uniaxial compression is a mixed shear and isotropic compression mode). There is also an effect from the friction between the particles and the base. The basal friction is small, and the change of the medium properties by replacing non-magnetic particles with magnetic particles is clear. The transition between these two response types as R_m varies is remarkably sharp, which means that near the transition, a dramatic change of the material response occurs with only a very small change in the fraction of magnetic particles.

Although the macroscopic response when magnetic particles are introduced changes significantly, as in Fig.3-

(a), the magnetic forces are very small ($< 0.05N$) compared to typical strong repulsive forces ($\sim 2N$) in the jammed state. Hence, the difference in P and Z induced by increasing R_m cannot be directly related to the weak magnetic forces. To understand the changes in material response with R_m we focus on the network structures formed by the magnetic disks. As shown in the inset of Fig.4-(b), neighbour magnetic particles tend to align in the same magnetic direction to attract each other, and hence to form magnetic chains. A pair of particles in a magnetic chain are identified as two nearby particles for which the distance between the ends of their magnetic bars is less than 3mm. These chains can consist of up to 12 particles, and can exhibit ramifications and loops (see inset of Fig.4-(b)). We define the length, ℓ , of a magnetic chain as the number of member particles, and we consider only chains that have $\ell \geq 3$. Fig.4-(a) shows the evolution of the probability density function (PDF), $P(\ell)$, for different compression steps for an $R_m = 100\%$ packing. The statistical distribution of ℓ is constant during the compression even if chains break and merge during the process (see video in supplementary material). $P(\ell)$ follows an exponential law with coefficient 0.72 ± 0.0115 :

$$P(\ell) = (2.0 \pm 0.013)e^{-0.72 \cdot \ell} \quad (1)$$

This statistical distribution remains the same within the errorbars for all $R_m > 0$ for the present experiments (not shown here).

This implies that whatever their density and the constraints inside the system, magnetic particles self-organize to maintain a magnetic chain network of the same statistical nature. Also, the average number of magnetic chains is roughly constant during the compression process but as shown in the inset of Fig.4-(a) it increases linearly with R_m .

The external load on a granular medium is not supported homogeneously by all the grains of the system but along forces chains forming a sparse network [18–20]. The force network presented as a black shadow in the inset of Fig.4-(b) is formed by particles having a G^2 value (averaged over all pixels inside the photo-elastic materials of the particle) higher than a certain threshold (8a.u., 60% of the maximum G^2 value in Fig.4-(b)) and in contact with other particles in the same situation. The threshold is far above the pressure that could result from magnetic interactions.

There are several seemingly contradictory facts that need explanation: 1) the magnetic forces are too small to directly affect the system response; 2) P and Z as functions of strain depend significantly on R_m ; 3) the magnetic particles self-organize into statistically stationary networks. A reasonable way for the magnetic particles to strongly affect the pressure, would be if they were associated with the strong force networks. To test this

hypothesis, we investigated the effect of the magnetic networks on the force network organization. Fig.4 (b) shows that when force chains begin to form, they grow preferentially along magnetic chains. We define R_1 to be the ratio of the number of particles in magnetic chains that are also in force chains to the number of particles in force chains. We compare this ratio to R_2 , defined as the ratio of particles in magnetic chains to all particles in the total system:

$$R_1 = \frac{\mathcal{N}(\text{particles in force \& magnetic chain})}{\mathcal{N}(\text{particles in force chains})} \quad (2)$$

$$R_2 = \frac{\mathcal{N}(\text{particles in magnetic chain})}{\text{total number of particles}}$$

Here, \mathcal{N} means particle number. If force chains form everywhere in the system without regard to magnetic chains, then those two ratios should be equal.

But as shown in Fig.4(b), initially, R_1 is much higher than ratio of magnetic chain particles in the total system: $R_1 \gg R_2$. Then the difference between both ratios vanishes when the pressure increases, and the network becomes denser after the jamming transition. This means that the first force chains of the granular material, which are the ones that constitute the backbone of the system and that will be the most loaded when the pressure increases, form mainly along the magnetic chains, whatever the ratio of magnetic particles.

Hence, the force chains that constitute the mechanical structure of a granular system under loading is imposed by a magnetic chain structure that itself self-organized and was statistically stationary during the evolution of the packing. The nearly binary response of the granular medium (like either the $R_m = 100\%$ or 0% responses) suggests that for low R_m , the density of magnetic chains, even if force chains form along them, is too low to be able to setup a strong structure and hence dominate the macroscopic response of the material. The sharp transition as R_m is varied smoothly (around $R_m = 50\%$) to a very different response strongly suggests a percolation transition. This property could be used to tune the rigidity of a granular material by changing the magnetic nature of a small number of grains. This tuning could be carried out by any process (e.g. temperature change, external magnetic field change) that would change the magnetic state of a small number of particles.

To conclude, we observe that even though the magnetic inter-particle force for our particles is much lower than typical jammed-state repulsive forces, the magnetic particles have an important impact on the response to compaction of the granular material, provided the fraction of magnetic particles is large enough. More precisely, a sharp transition, that we believe can be mapped to a percolation transition in the pressure/coordination-strain/packing fraction curves, is observed around $R_m \simeq 50\%$. Also, self-organized magnetic chains occur in the

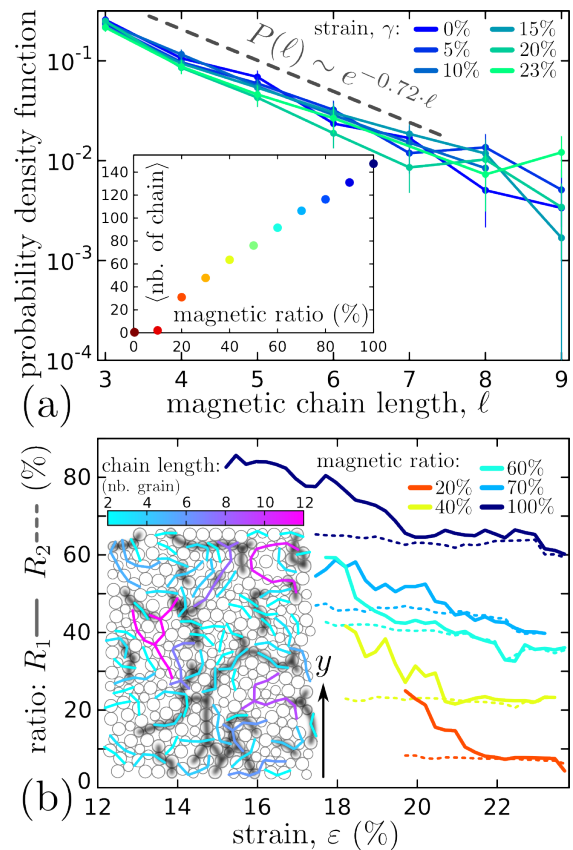


FIG. 4. (color online) (a): probability density function (PDF) of the length, ℓ , of magnetic chains, averaged over 3 100% magnetic particle experiments measured at different steps of the compression. Even if chains break and merge, the PDF still follows an exponential law (grey dashed line) with coefficient 3.2 ± 0.15 . (a)-Inset: average number of magnetic chains for experiments with different percentage of magnetic particles. For each point, the average is done over all the compression steps for 3 runs with the same R_m . The standard deviation is too small to be visible on the graph. (b): Evolution of the ratios R_1 (plain line, ratio of particles in a magnetic chain among particles in a force chain) and R_2 (dashed line, ratio of particles in a magnetic chain in the whole system) during the compression for different mixes of magnetic particles. Force chains mainly follow magnetic chains (see text for details). (b)-inset: part of the system for a 100% magnetic particle experiment with $\varepsilon = 16\%$, colored lines show magnetic chains (color scale for length) and dark lines shadow show force chains.

packing at a very early stage. Even though the magnetic chains evolve during compression (breaking, merging) the statistics of their length remain the same throughout the process. This last point helps explain the first one, since we observe that force chains that support the applied load are formed preferentially along the magnetic chains, particularly for smaller strains. When the magnetic chain fraction is too low, they cannot impose a mechanical network that is strong enough to affect the macroscopic behavior of the granular material. We believe this property

can be used in novel applications.

Acknowledgements: This work was supported by The NSF-Research Triangle MRSEC, NSF grant DMR-1206351, The William M. Keck Foundation, and a London post-doctoral fellowship for JB.

-
- [1] A. J. Liu and S. R. Nagel. Nonlinear dynamics: Jamming is not just cool any more. *Nature*, 396(6706):21–22, 1998.
- [2] K. Dierichs and A. Menges. Aggregate structures: Material and machine computation of designed granular substances. *Architectural Design*, 82(2):74–81, 2012.
- [3] E. Brown, N. Rodenberg, J. Amend, A. Mozeika, E. Steltz, M. R. Zakin, H. Lipson, and H. M. Jaeger. Universal robotic gripper based on the jamming of granular material. *Proceedings of the National Academy of Sciences*, 107(44):18809–18814, 2010.
- [4] N. G. Cheng, M. B. Lobovsky, S. J. Keating, A. M. Setapen, K. I. Gero, A. E. Hosoi, and K. D. Iagnemma. Design and analysis of a robust, low-cost, highly articulated manipulator enabled by jamming of granular media. In *Robotics and Automation (ICRA), 2012 IEEE International Conference on*, pages 4328–4333, May 2012.
- [5] E. Steltz, A. Mozeika, M. Rodenberg, E. Brown, and H. M. Jaeger. Jsel: Jamming skin enabled locomotion. In *Intelligent Robots and Systems, 2009. IROS 2009. IEEE/RSJ International Conference on*, pages 5672–5677, Oct 2009.
- [6] H. M. Jaeger. Celebrating soft matter’s 10th anniversary: Toward jamming by design. *Soft Matter*, 11:12–27, 2015.
- [7] M. Z. Miskin and H. M. Jaeger. Adapting granular materials through artificial evolution. *Nature materials*, 12(4):326–331, 2013.
- [8] A. G. Athanassiadis, M. Z. Miskin, P. Kaplan, N. Rodenberg, S. H. Lee, J. Merritt, E. Brown, J. Amend, H. Lipson, and H. M. Jaeger. Particle shape effects on the stress response of granular packings. *Soft Matter*, 10:48–59, 2014.
- [9] K. D. Weiss, J. D. Carlson, and D. A. Nixon. Viscoelastic properties of magneto-and electro-rheological fluids. *Journal of Intelligent Material Systems and Structures*, 5(6):772–775, 1994.
- [10] M. Hagenbüchle and J. Liu. Chain formation and chain dynamics in a dilute magnetorheological fluid. *Applied Optics*, 36(30):7664–7671, Oct 1997.
- [11] T. Ukai and T. Maekawa. Patterns formed by paramagnetic particles in a horizontal layer of a magnetorheological fluid subjected to a dc magnetic field. *Physical Review E*, 69:032501, Mar 2004.
- [12] Smooth-On. Star-mold[®] 15 (slow).
- [13] Smooth-On. Clear-flex[®] 50.
- [14] D. Howell, R. P. Behringer, and C. Veje. Stress fluctuations in a 2d granular couette experiment: A continuous transition. *Physical Review Letter*, 82:5241–5244, Jun 1999.
- [15] Junfei Geng, D. Howell, E. Longhi, R. P. Behringer, G. Reydellet, L. Vanel, E. Clément, and S. Luding. Footprints in sand: The response of a granular material to local perturbations. *Physical Review Letter*, 87:035506, Jul 2001.
- [16] J. Ren, J. A. Dijksman, and R. P. Behringer. Reynolds pressure and relaxation in a sheared granular system. *Physical Review Letter*, 110:018302, Jan 2013.
- [17] R. P. Behringer, D. Bi, B. Chakraborty, A. Clark, J. A. Dijksman, J. Ren, and J. Zhang. Statistical properties of granular materials near jamming. *Journal of Statistical Mechanics: Theory and Experiment*, 2014(6):P06004, 2014.
- [18] T. S. Majmudar, M. Sperl, S. Luding, and R. P. Behringer. Jamming transition in granular systems. *Physical Review Letters*, 98:058001, Jan 2007.
- [19] F. Radjai, D. E. Wolf, M. Jean, and J.-J. Moreau. Bimodal character of stress transmission in granular packings. *Physical Review Letters*, 80:61–64, Jan 1998.
- [20] L. Kondic, A. Goulet, C. S. O’Hern, M. Kramar, K. Mischaikow, and R. P. Behringer. Topology of force networks in compressed granular media. *Europhysics Letters*, 97(5):54001, 2012.